"From discrete to continuum models of three-dimensional deformations in epithelial sheets" Supporting Information

N. Murisic, V. Hakim, I. Kevrekidis, S. Y. Shvartsman and B. Audoly

July 15, 2015

S1 Detailed derivation of the homogenized plate model

We show that the energy of the vertex model introduced in the main text,

$$\mathcal{E}_{\rm vm} = \frac{1}{2}\sum_f (A_f - 1)^2 + G\sum_e L_e + \frac{H}{2}\sum_f {P_f}^2 + B\sum_{e'}(1 - \mathbf{N}_{f_1(e')}\cdot\mathbf{N}_{f_2(e')}), \tag{1}$$

is equivalent in the smooth limit to a plate energy, $\mathcal{E}_{\rm vm} \approx \mathcal{E}_{\rm plate}$, where

$$\mathcal{E}_{\rm plate} = \frac{1}{2}\iint \left(\lambda\ \mathrm{tr}^2\,\mathbf{E} + 2\,\mu\,|\mathbf{E}^2| + \beta\,(\Delta w)^2\right)\,\mathrm{d}X\,\mathrm{d}Y, \tag{2}$$

up to constant terms which we can ignore. We refer the reader to the main text for a definition of the various quantities entering in the vertex model. In the equivalent plate model, $\mathbf{E}$ is a macroscopic measure of stretching strain, see equation (14) below, w is the deflection and Δw is its Laplacian with respect to the Lagrangian coordinates (X, Y). The Lamé parameters λ and μ characterize the stretching behavior of the equivalent plate (μ being the shear modulus), and β is a bending modulus. These three parameters are expressed below in terms of the original parameters G, H and B, by identifying the two energies in the continuous limit.

In what follows, we omit the details of the calculations. They have been carried out using the symbolic calculation language Wolfram Mathematica [8]. The source code (notebook) is appended at the end of this document.

S1.1 Harmonic macroscopic and microscopic displacement (Cauchy-Born rule)

Let $\mathbf{X} = (X, Y)$ be the coordinates in reference configuration '0' of a vertex. Its position $\mathbf{x}$ in actual configuration is first scaled with ratio a, and then moved by a small macroscopic displacement plus a small microscopic displacement, see figure S1. The role of the uniform scaling is to relax the in-plane stress present in the configuration of reference, yielding the intermediate configuration 'PE' shown in the figure.

The Cauchy-Born rule provides a starting point for deriving a continuum description of lattices whose energy is the sum of interactions between neighbors. For simple Bravais lattices, the standard Cauchy-Born rule applies: a homogeneous deformation is applied onto the lattice. The hexagonal lattice, however, is a multi-lattice as it can be viewed as the union of *two* simple Bravais lattices. Therefore, the standard Cauchy-Born rule must be modified, see for instance [4]: a homogeneous deformation must be applied to each sub-lattice (with the same deformation gradient for all sub-lattices) and in addition, *a shift between them must be allowed*. This shift, called inner displacement, gives rise to an oscillatory displacement field which we refer to as the *microscopic displacement*. This shift is required for the equilibrium of all vertices to be satisfied. This approach based on homogeneous transformations works well when the energy of the

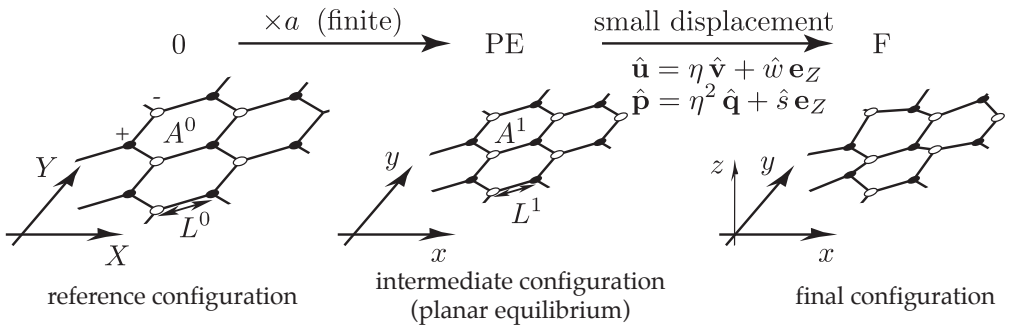

Figure S1: Analysis of the 3D vertex model combines a uniform scaling with ratio $a < 1$ from the reference configuration '0', and a small perturbation. The vertices are represented by filled and open disks depending on which Bravais sublattice they belong to. In the intermediate state 'PE', the edge length is $L^1 = a\,L^0$ and the face area is $A^1 = a^2\,A^0$. Using homogenization techniques, the energy of the final configuration 'F' given by the 3D vertex model (1) is identified to the energy of a thin elastic plate.

continuous model is a function of the deformation gradient only. To capture the higher-order derivatives associated with bending, extensions of the Cauchy-Born rule have been proposed [1, 2, 9]. Here, we propose a simpler approach, and assume that the displacement of the vertices belonging to each sub-lattice are harmonic functions of the position with a long wavelength. When combined with appropriate scaling assumptions on the large wavelength and on the small displacement, this makes the bending term appear naturally, as we show below. Another benefit of this approach is that it easily handles the dot product of unit normals in the bending term, even though this term cannot be easily written as a standard interaction term depending on the distances between neighboring vertices.

We assume that both the macroscopic and microscopic displacements are harmonic functions of the coordinates, see equation (5) in the main text:

$$\mathbf{x} = a\,\mathbf{X} + \Re\left(\left(\hat{\mathbf{u}} \pm \frac{\hat{\mathbf{p}}}{2}\right) e^{i\,\eta\,\mathbf{K}\cdot\mathbf{X}}\right). \tag{3}$$

Here, $\Re$ denotes the real part, $\mathbf{K} = (K_x, K_y)$ is a planar vector, η is a small real expansion parameter, $\mathbf{k} = \eta\,\mathbf{K}$ is the wavevector of the perturbation, and hats denote complex quantities: $\hat{\mathbf{u}}$ is a complex vector of dimension 3 representing the (smooth) macroscopic displacement, $\hat{\mathbf{p}}$ is a complex vector of dimension 3 representing the (oscillatory) microscopic displacement. The sign '$\pm$' is different for each sub-lattice: it is '$+$' for vertices marked with filled disks in figure S1, and '$-$' for vertices marked with open disks. As a result, the two sublattices are shifted with respect to one another by a microscopic shift vector $\Re\left(\hat{\mathbf{p}}\,e^{i\,\eta\,\mathbf{K}\cdot\mathbf{X}}\right)$.

In what follows, we consider the continuous limit $\eta \to 0$, where both the macroscopic displacement $\hat{\mathbf{u}}$ and the shift $\hat{\mathbf{p}}$ vary on a length-scale that is large compared to the mesh size. This is the asymptotic regime where the vertex model converges to a plate model.

The X and Y components of the complex amplitude vectors $\hat{\mathbf{u}}$ and $\hat{\mathbf{p}}$ correspond to in-plane perturbations, and their Z component to out-of-plane perturbations. For the energy to converge in the limit $\eta \to 0$, we need to make some scaling assumptions on these complex amplitudes. These read

$$\hat{\mathbf{u}} = \eta\,\hat{\mathbf{v}} + \hat{w}\,\mathbf{e}_Z \quad \text{and} \quad \hat{\mathbf{p}} = \eta^2\,\hat{\mathbf{q}} + \eta^2\,\hat{s}\,\mathbf{e}_Z \tag{4a}$$

where

$$\hat{\mathbf{v}} = \hat{v}_X\,\mathbf{e}_X + \hat{v}_Y\,\mathbf{e}_Y \quad \text{and} \quad \hat{\mathbf{q}} = \hat{q}_X\,\mathbf{e}_X + \hat{q}_Y\,\mathbf{e}_Y \tag{4b}$$

and $(\mathbf{e}_X, \mathbf{e}_Y, \mathbf{e}_Z)$ denotes the Cartesian basis. We have assumed that the in-plane projection of $\hat{\mathbf{u}}$ scales like η, that its out-of-plane projection $\hat{w}$ is independent of η, and that both components of $\hat{\mathbf{q}}$ scale like η^2. As we shall see, these scaling assumptions allow the various contributions entering in the strain measures to

be balanced. They are moreover natural in the context of the vertex model, and are similar to the scaling assumptions underlying the classical theory of plates, see for instance [3].

S1.2 Expansion of the energy of a single cell

The energy (1) can be rewritten as a sum over all cells of an energy per cell, $\mathcal{E}_{\rm vm} = \sum_f \epsilon_f$, where

$$\epsilon_f = \frac{1}{2}(A_f - 1)^2 + \frac{G}{2}\, P_f + \frac{H}{2} {P_f}^2 + \frac{B}{2} \sum_{\langle f, f' \rangle} (1 - \mathbf{N}_f \cdot \mathbf{N}_{f'}). \tag{5}$$

On the right-hand side, the sum runs over all faces f' adjacent to f. Note the division by 2 in the G and B terms, which comes from the fact that a given edge belongs to two faces, and is therefore counted twice when summing over all faces.

To homogenize the vertex model, we consider the energy $\epsilon_{f=0}$ of the face $f = 0$ centered at the origin $(X, Y) = (0, 0)$ in the limit $\eta \to 0$, and derive an asymptotic expression of $\epsilon_{f=0}$ as a function of the rescaled wavevector $\mathbf{K}$, of the rescaled complex in-plane displacement $\hat{\mathbf{v}}$ and of the complex out-of-plane displacement $\hat{w}$.

In reference configuration, the vertices $\mathbf{X}_j$ of the face $f = 0$ are

$$\mathbf{X}_j = L^0\, (\cos\theta_j, \sin\theta_j, 0)$$

where $1 \leq j \leq 6$ is an integer and $\theta_j = (2\,j + 1)\,\frac{\pi}{6}$; the reference position of the vertices of the adjacent cells are calculated similarly. Using equations (3–4), one can calculate the position $\mathbf{x}_j$ of all vertices belonging to the central cells and to its adjacent cells in actual configuration as a function of j, a, η, $\mathbf{K}$, $\hat{\mathbf{v}}$, $\hat{\mathbf{q}}$, $\hat{w}$ and $\hat{s}$. One can then calculate all the quantities entering in the definition of the energy as follows (see main text for their definition): one expresses the area vector $\mathbf{A}_f$, the scalar area A_f and the unit normal $\mathbf{N}_f$ for the central cell $f = 0$ and its adjacent cells. Inserting into equation (5), we obtain the expression of the energy of the face $f = 0$, $\epsilon_{f=0}(a, \eta, \mathbf{K}, \hat{\mathbf{v}}, \hat{\mathbf{q}}, \hat{w}, \hat{s})$.

Next, we expand this expression of $\epsilon_{f=0}$ in a series with respect to η up to fourth order. Doing this calculation by hand is tedious. We carried it out using the symbolic calculation language Wolfram Mathematica [8]. The result is

$$\begin{aligned}
\epsilon_{f=0}(a, \eta, \mathbf{K}, \hat{\mathbf{v}}, \hat{\mathbf{q}}, \hat{w}, \hat{s}) = \epsilon_{\rm PE}(a) + \frac{\epsilon'_{\rm PE}(a)}{2\,a} \Bigg\{ & - a\, \mathbf{K} \cdot \mathbf{v}_{\rm im} + \frac{1}{2}\, |\mathbf{K}|^2\, w_{\rm im}^2 \Bigg\} \eta^2 \cdots \\
& + \Bigg\{ \frac{\epsilon'_{\rm PE}(a)}{24\,\sqrt{3}} \left[|\mathbf{K}|^2\, \mathbf{K} \cdot \mathbf{v}_{\rm im} - \frac{|\mathbf{K}|^4}{a}\, w_{\rm im}^2 + \frac{3^{3/4}}{\sqrt{2}}\, \mathbf{q}_{\rm re} \cdot \mathcal{S} : (\mathbf{K} \otimes \mathbf{K}) \right] + \frac{2\,a^2 - \tilde{G}}{4}\, (\mathbf{K} \cdot \mathbf{v}_{\rm im})^2 \cdots \\
& + \left(\frac{1}{4}\, \tilde{G} + \sqrt{3}\, H \right) \left[\frac{3}{2}\, |\mathbf{K}|^2\, |\mathbf{v}_{\rm im}|^2 + 3\,\sqrt{3}\, (|\mathbf{q}_{\rm re}|^2 + 2\, s_{\rm re}^2) + \sqrt{2}\, 3^{3/4}\, \mathbf{q}_{\rm re} \cdot \mathcal{S} : \left(\mathbf{K} \otimes \left(\mathbf{v}_{\rm im} - \frac{w_{\rm im}^2}{2\,a}\, \mathbf{K} \right) \right) \right] \cdots \\
& + \frac{1 - \frac{3}{4}\, \tilde{G} - \sqrt{3}\, H}{8\, a^2} \left(-4\, a\, |\mathbf{K}|^2\, \mathbf{K} \cdot \mathbf{v}_{\rm im}\, w_{\rm im}^2 + |\mathbf{K}|^4\, w_{\rm im}^4 \right) + \frac{\frac{1}{4}\, \tilde{G} + \sqrt{3}\, H + 6\, \frac{B}{a^2}}{4\,\sqrt{3}}\, |\mathbf{K}|^4\, w_{\rm re}^2 \Bigg\} \eta^4 + \mathcal{O}(\eta^6)
\end{aligned} \tag{6}$$

where $\mathbf{v}_{\rm im} = \Im(\hat{\mathbf{v}})$, $w_{\rm im} = \Im(\hat{w})$ (the subscript 'im' and the operator $\Im$ denote the imaginary part), $\mathbf{q}_{\rm re} = \Re(\hat{\mathbf{q}})$, $w_{\rm re} = \Re(\hat{w})$, $s_{\rm re} = \Re(\hat{s})$ (the subscript 're' and the operator $\Re$ denote the real part), $\tilde{G}$ is a shorthand for

$$\tilde{G} = \frac{\sqrt[4]{3}\, G}{\sqrt{2}\, a}, \tag{7}$$

and the constant term $\epsilon_{\rm PE}(a)$ denotes the energy of the intermediate configuration 'PE' (uniform scaling transformation with ratio a):

$$\epsilon_{\rm PE}(a) = \frac{1}{2}\, (1 - a^2)^2 + a^2\, (2\,\tilde{G} + 4\,\sqrt{3}\, H), \tag{8}$$

see also equation (6) in the main text.

In equation (6), we have also introduced a tensor of rank 3 living in the tangent plane (X, Y). It is defined in terms of the matrices $\mathbf{S}_X$ and $\mathbf{S}_Y$ obtained by fixing the first index: $\mathcal{S} = \mathbf{e}_X \otimes \mathbf{S}_X + \mathbf{e}_Y \otimes \mathbf{S}_Y$ where

$$\mathbf{S}_X = \begin{pmatrix} \mathcal{S}_{XXX} & \mathcal{S}_{XXY} \\ \mathcal{S}_{XYX} & \mathcal{S}_{XYY} \end{pmatrix} = \begin{pmatrix} 0 & 1 \\ 1 & 0 \end{pmatrix} \quad \text{and} \quad \mathcal{S}_Y = \begin{pmatrix} \mathcal{S}_{YXX} & \mathcal{S}_{YXY} \\ \mathcal{S}_{YYX} & \mathcal{S}_{YYY} \end{pmatrix} = \begin{pmatrix} 1 & 0 \\ 0 & -1 \end{pmatrix} \tag{9}$$

We shall refer to $\mathbf{S}_X$ and $\mathbf{S}_Y$ as the *spin matrices*. Note that these matrices are symmetric, and such that $\mathbf{S}_X^2 = \mathbf{S}_Y^2 = \mathbf{I}_2$ where $\mathbf{I}_2$ is the identity matrix in dimension 2. In equation (6), the triple contraction of $\mathcal{S}$ is defined by

$$\mathbf{q}_{\mathrm{re}} \cdot \mathcal{S} : \mathbf{A} = \sum_{i,j,k \in \{X,Y\}} q^i_{\mathrm{re}} \mathcal{S}_{ijk} A_{jk} = q^X_{\mathrm{re}}\, \mathbf{S}_X : \mathbf{A} + q^Y_{\mathrm{re}}\, \mathbf{S}_Y : \mathbf{A} \tag{10}$$

where q^i_{re}, $\mathcal{S}_{ijk}$, and A_{jk} denote the components of the vector $\mathbf{q}_{\mathrm{re}}$, of the tensor $\mathcal{S}$ and of the matrix $\mathbf{A}$ in the Cartesian basis $(\mathbf{e}_X, \mathbf{e}_Y)$, respectively. Since $\mathcal{S}$ is symmetric with respect to its last two indices, the pairing of indices in the double contraction on the right-hand side is unimportant.

Note that the right-hand side of equation (6) involves only scalar invariants built from the vectors $\mathbf{K}$, $\mathbf{v}_{\mathrm{im}}$ and $\mathbf{q}_{\mathrm{re}}$, and from the tensor $\mathcal{S}$.

S1.3 Macroscopic strain measures

Our goal is now to identify the strain quantities relevant to the theory of thin plates, namely the stretching strain and the mean curvature, in the right-hand side of equation (6). We start by the macroscopic stretching strain. Let us first define the macroscopic displacement $\mathbf{x}_{\mathrm{macro}}$, obtained by averaging out the microscopic displacement from equation (3):

$$\mathbf{x}_{\mathrm{macro}} = a\, \mathbf{X} + \Re\left(\hat{\mathbf{u}}\, e^{i\, \eta\, \mathbf{K}\cdot\mathbf{X}}\right) \tag{11}$$

The corresponding deformation gradient reads

$$\mathbf{F}_{\mathrm{macro}} = \frac{\partial \mathbf{x}_{\mathrm{macro}}}{\partial \mathbf{X}}. \tag{12}$$

The stretching strain is given by the (macroscopic) Cauchy-Green tensor $\mathbf{E}$ which we define by

$$\mathbf{E} = \frac{1}{2\, a}\, \left(\mathbf{F}^T_{\mathrm{macro}} \cdot \mathbf{F}_{\mathrm{macro}} - a^2\, \mathbf{I}_2\right). \tag{13}$$

This definition is such that $\mathbf{E} = \mathbf{0}$ in the intermediate configuration 'I'. The prefactor $1/(2\, a)$ warrants that that $\mathrm{tr}\, \mathbf{E}$ can be interpreted as the relative increase of area from the intermediate configuration, in the linear case (see below). Note that the dimension of $\mathbf{E}$ is 2×2.

To gain some insight into the Cauchy-Green tensor, we derive its explicit expression when the incremental macroscopic displacement (v_X, v_Y, w) is a generic function, *i.e.* when the final position is $\mathbf{x}_{\mathrm{macro}} = a\, \mathbf{X} + v_X(\mathbf{X})\, \mathbf{e}_X + v_Y(\mathbf{X})\, \mathbf{e}_Y + w(\mathbf{X})\, \mathbf{e}_Z$. Inserting into equation (13), we find

$$E_{ij} = \frac{v_{j,i} + v_{i,j}}{2} + \frac{1}{2\, a}\, v_{k,i}\, v_{k,j} + \frac{1}{2\, a}\, w_{,i}\, w_{,j}, \tag{14}$$

where indices (i, j, k) run over the in-plane directions X and Y, a comma in subscript stands for a partial derivative, and we use the Einstein summation convention. The first term on the right-hand side is the linear strain, the second term can be neglected in buckling analysis (the Föppl-von Kàrmàn approximation of the strain) and the last non-linear term couples stretching with the deflection w.

Returning to the special Fourier form (3) of the displacement and to our scaling assumption (4), we write the macroscopic deformation gradient at the origin $(X, Y) = (0, 0)$ as

$$\mathbf{F}_{\mathrm{macro}}(0,0) = \left.\frac{\partial \mathbf{x}_{\mathrm{macro}}}{\partial \mathbf{X}}\right|_{\mathbf{X}=\mathbf{0}} = a\, \mathbf{I}_{3\times 2} + \Re(\hat{\mathbf{u}} \otimes i\, \eta\, \mathbf{K}) = a\, \mathbf{I}_{3\times 2} - (\eta\, \mathbf{v}_{\mathrm{im}} + w_{\mathrm{im}}\, \mathbf{e}_Z) \otimes \eta\, \mathbf{K}, \tag{15}$$

where $\mathbf{I}_{3\times 2}$ is the matrix of size 3×2 obtained by appending a zero row at the bottom of the identity matrix $\mathbf{I}_2$, and $\otimes$ denotes the outer product of vectors.

The corresponding macroscopic Cauchy-Green strain tensor reads, by equation (13),

$$\mathbf{E}(0,0) = -\eta\,\mathbf{v}_{\rm im}\odot\eta\,\mathbf{K} + \frac{\eta\,\mathbf{K}\otimes\eta\mathbf{K}}{2\,a}\,(\eta^2\,|\mathbf{v}_{\rm im}|^2 + w_{\rm im}^2), \tag{16}$$

where $\mathbf{a}\odot\mathbf{b} = \frac{\mathbf{a}\otimes\mathbf{b}+\mathbf{b}\otimes\mathbf{a}}{2}$ denotes the symmetrized outer product. This equation is a variant of equation (14) in tensor notation.

We now proceed to calculate the mean curvature. We denote by Δ the Laplacian operator with respect to the reference coordinates (X,Y), $\Delta = \frac{\partial^2}{\partial X^2} + \frac{\partial^2}{\partial Y^2}$. The mean curvature is given in terms of the Laplacian of the deflection $\mathbf{x}_{\rm macro}\cdot\mathbf{e}_Z = \Re(\hat{w}\,e^{i\,\eta\,\mathbf{K}\cdot\mathbf{X}})$ as

$$\frac{1}{2\,a^2}\,\Delta w(0,0) = \frac{1}{2\,a^2}\,\Delta[\Re(\hat{w}\,e^{i\,\eta\,\mathbf{K}\cdot\mathbf{X}})]_{\mathbf{X}=\mathbf{0}} = -\frac{1}{2\,a^2}\,|\eta\,\mathbf{K}|^2\,w_{\rm re}. \tag{17}$$

The coefficient a^2 in the denominator converts the Laplacian Δ with respect to the Lagrangian coordinates, to a Laplacian with respect to the coordinates in the intermediate configuration 'PE'.

We now proceed to rewrite the expansion (6) in terms of the Cauchy-Green strain and the mean curvature, see equations (16–17).

S1.4 Stretch in intermediate configuration

We observe that the η^2 term in the expansion (6) involves the trace of the Cauchy-Green tensor:

$$\epsilon_{f=0}(a,\eta,\mathbf{K},\hat{\mathbf{v}},\hat{\mathbf{q}},\hat{w},\hat{s}) = \epsilon_{\rm PE}(a) + \epsilon'_{\rm PE}(a)\,\frac{\operatorname{tr}\mathbf{E}(0,0)}{2} + \mathcal{O}(\eta^4), \tag{18}$$

where $\mathbf{E}(0,0) = \mathcal{O}(\eta^2)$. This term cancels by the condition

$$\epsilon'_{\rm PE}(a) = 0. \tag{19}$$

This expression defines (implicitly) the stretch a in the intermediate configuration making the energy stationary, *i.e.* relaxing the in-plane stretch.

To derive the plate model, we will need to analyze the next order in the expansion, η^4.

S1.5 Continuous energy as a function of microscopic shift

We can now simplify the energy of the vertex model in equation (6) in two ways: we use the implicit equation (19) for a, which allows to get rid of the two terms proportional to $\epsilon'_{\rm PE}(a)$, and we rewrite the remaining terms using the macroscopic Cauchy-Green tensor $\mathbf{E}(0,0)$ and the mean curvature calculated in §S1.3.

With the help of the symbolic calculation language Wolfram Mathematica (see the companion notebook for details), we find

$$\begin{aligned}\epsilon_{f=0}(a,\eta,\mathbf{K},\hat{\mathbf{v}},\hat{\mathbf{q}},\hat{w},\hat{s}) = \epsilon_{\rm PE}(a) + \frac{\lambda_*}{2}\,\operatorname{tr}^2\mathbf{E}(0,0) + \mu_*\,|\mathbf{E}(0,0)|^2 + \frac{\beta}{2}\,\big(\Delta w(0,0)\big)^2\cdots\\ + \frac{\tau}{2}\,\eta^4\,\big(|\mathbf{q}(0,0)|^2 + 2\,s^2(0,0)\big) - \gamma\,\eta^2\,\mathbf{q}(0)\cdot\mathcal{S}:\mathbf{E}(0,0) + \mathcal{O}(\eta^6)\end{aligned} \tag{20}$$

where $|\mathbf{E}^2| = \mathbf{E}:\mathbf{E} = \operatorname{tr}(\mathbf{E}\cdot\mathbf{E})$, and $\mathbf{q}(0,0)$ and $s(0,0)$ denote the scaled tangent and normal components of the microscopic displacement at the origin, $\mathbf{q}(0,0) = \Re(\hat{\mathbf{q}}) = \mathbf{q}_{\rm re}$ and $s(0,0) = \Re(\hat{s}) = s_{\rm re}$. The moduli are

found by this identification as

$$\lambda_* = 1 - \frac{9}{4}\,(1 - a^2) + 2\,\sqrt{3}\,H \tag{21a}$$

$$\mu_* = \frac{3}{4}\,(1 - a^2) \tag{21b}$$

$$\beta = \frac{1 - a^2}{8\,\sqrt{3}} + \frac{\sqrt{3}}{a^2}\,B \tag{21c}$$

$$\tau = \frac{3\,\sqrt{3}}{2}(1 - a^2) \tag{21d}$$

$$\gamma = \frac{3^{3/4}}{2\,\sqrt{2}}\,(1 - a^2). \tag{21e}$$

The first line in equation (20) defines a smooth plate model, compare with equation (2). However, we must take care of the other terms involving the microscopic displacement (see below) before we can derive the equivalent plate model.

Note that $\mathbf{E}(0,0)$ and $\Delta w(0,0)$ are quantities of order η^2, see equations (16) and (17): except for the constant term $\epsilon_{\mathrm{PE}}(a)$, all terms on the right-hand side of equation (20) are of order η^4. This justifies the scaling assumptions proposed in §S1.1.

Note that both sides of equation (20) are evaluated at the central cell, $f = 0$, which, in the continuous description, is used as the origin of the axes $(X, Y) = (0, 0)$; this is consistent.

S1.6 Relaxed continuous energy

The microscopic shift $\mathbf{p}(0,0) = \eta^2\,(\mathbf{q}(0,0) + s(0,0)\,\mathbf{e}_Z)$ between the two Bravais sublattices is found by minimizing the continuous energy appearing on the right-hand side of equation (20). We observe that $s(0,0)$ appears only in the form $s^2(0,0)$ in the τ-term. This term is minimum for

$$s(0,0) = 0, \tag{22}$$

and we conclude that the microscopic shift vector is in-plane.

The scaled in-plane component $\mathbf{q}$ of the microscopic shift $\mathbf{p}$ appears in the two last terms of equation (20). The stationarity condition of this right-hand side reads $\tau\,\eta^4\,\mathbf{q}(0,0) - \gamma\,\eta^2\,\mathcal{S} : \mathbf{E}(0,0)$. Therefore, the microscopic shift reads

$$\mathbf{p}(0,0) = \eta^2\,\mathbf{q}(0,0) = \frac{\gamma}{\tau}\,\mathcal{S} : \mathbf{E}(0,0), \tag{23}$$

where the tensor $\mathcal{S}$, of rank 3, has been defined in equation (9). This important relation yields the microscopic shift $\mathbf{p}$ in terms of the macroscopic Cauchy-Green tensor $\mathbf{E}$. It has been established for the central cell $f = 0$ lying at the origin of the coordinate system $(X, Y) = (0, 0)$ but is obviously valid everywhere. Therefore we drop the coordinates $(0, 0)$.

Inserting this optimal value of the shift $\mathbf{q}$ into the energy terms written on the second line of equation (20), we have

$$\frac{\tau}{2}\,\eta^4\,\left(|\mathbf{q}|^2 + 2\,s^2\right) - \gamma\,\eta^2\,\mathbf{q}\cdot\mathcal{S} : \mathbf{E} = \frac{\tau}{2}\,|\mathbf{p}|^2 - \gamma\,\mathbf{p}\cdot\mathcal{S} : \mathbf{E} = -\frac{\gamma^2}{2\,\tau}\,\left(\mathcal{S} : \mathbf{E}\right)^2$$

This expression can be further simplified by using the expressions for τ and γ in equation (21) and the identity $(\mathcal{S} : \mathbf{E})^2 = -\,\mathrm{tr}^2\,\mathbf{E} + 2\,|\mathbf{E}|^2$ (which can easily be established for any symmetric matrix $\mathbf{E}$ using the definition of the tensor $\mathcal{S}$):

$$\frac{\tau}{2}\,\eta^4\,\left(|\mathbf{q}|^2 + 2\,s^2\right) - \gamma\,\eta^2\,\mathbf{q}\cdot\mathcal{S} : \mathbf{E} = \frac{1 - a^2}{4}\,\left(\frac{\mathrm{tr}^2\,\mathbf{E}}{2} - |\mathbf{E}|^2\right) \tag{24}$$

Inserting this into the right-hand side of equation (20), we find the relaxed energy as

$$\epsilon_{f=0}^{\mathrm{relaxed}}(a, \eta, \mathbf{K}, \hat{\mathbf{v}}, \hat{w}) = \epsilon_{\mathrm{PE}}(a) + \frac{\lambda}{2}\,\mathrm{tr}^2\,\mathbf{E}(0,0) + \mu\,|\mathbf{E}(0,0)|^2 + \frac{\beta}{2}\,\left(\Delta w(0,0)\right)^2 + \mathcal{O}(\eta^6) \tag{25}$$

where the new elastic moduli effectively capture the microscopic field,

$$\lambda = \lambda_* + \frac{1-a^2}{4} = -1 + 2\,a^2 + 2\,\sqrt{3}\,H \tag{26a}$$

$$\mu = \mu_* - \frac{1-a^2}{4} = \frac{1}{2}\,(1-a^2) \tag{26b}$$

$$\beta = \qquad\qquad \frac{1-a^2}{8\,\sqrt{3}} + \frac{\sqrt{3}}{a^2}\,B. \tag{26c}$$

Here, λ and μ are Lamé parameters for stretching (μ is a shear modulus), and β is the bending modulus.

Summing equation (25) over all cells, we obtain the total energy of the vertex model on the left-hand side, and the energy of a continuous plate model on the right-hand side,

$$\mathcal{E}_{\rm vm} = \mathcal{E}_{\rm plate} + A\,\epsilon_{\rm PE}(a) + \mathcal{O}(\eta^6), \tag{27}$$

where $A = \iint \mathrm{d}X\,\mathrm{d}Y$ is the undeformed domain area. Note that all cells have a unit area in reference configuration and, as a result, a sum over cells is equivalent in the smooth limit to an integral over the reference domain.

Equation (27) establishes the asymptotic equivalence of the discrete vertex model and of the continuous plate model for any long-wavelength harmonic perturbation (up to an unimportant constant term). By the principle of linear superposition, the equivalence between these linear models holds for an arbitrary long-wavelength perturbation. At this order in the expansion, the hexagonal lattice is effectively isotropic.

S1.7 Material stability

In 2D, the thermodynamic stability requires that the Lamé parameters λ and μ appearing in the stretching term in equation (26a–26b) satisfy $\mu > 0$ and $\lambda + \mu \geq 0$: $\mu = 0$ corresponds to the minimum possible Poisson's ratio $\nu = -1$, while $\lambda + \mu = 0$ corresponds to its maximum $\nu = 1$ (area-preserving material in 2D). For a fixed value of (G, H), only the roots a of equation (19) satisfying these conditions must be considered — if they exist. For a thorough discussion of stability of hexagonal solutions of the vertex model, see [6]. In the case $H = 0$ considered in our numerical study, Eq. (7) of the main text reads $\tilde{G} = 1 - a^2$ when expressed in terms of the quantity $\tilde{G}$ defined above in equation (7): the two stability conditions, $\mu > 0$ and $\lambda + \mu \geq 0$, correspond to $1/\sqrt{3} \leq a < 1$, *i.e.* $0 < G < 2^{3/2}/3^{7/4} \approx 0.4136$.

S1.8 Comparison to the moduli derived by Staple et al.

Our expressions in Eq. 7 of the main text correct those derived by Staple et al. [6], as we explain here.

The equation 15 in [6], gives what the authors call a *shear modulus* $\overline{\mu}$ and a *compression modulus* $\overline{\lambda}$. When converted to our notation, they read $\overline{\mu} = \lambda + \mu$ and $\overline{\lambda} = 2\,\mu$. These expressions need to be corrected as follows. Their moduli have been mixed up: $\overline{\lambda}$ is actually proportional to the shear modulus μ (and not to the compression modulus) and $\overline{\mu}$ to the bulk modulus $K = \lambda + \mu$ (and not to the shear modulus). Their shear modulus $\overline{\lambda}$ is off by an extra factor 2, an error that can be traced back to their equation 13: on the right-hand side of this equation, the factor 1/2 should read 1/4. With these corrections, their moduli agree with our λ_* and μ_* appearing in equations (21a–21b).

Still, these moduli are unphysical, as they ignore the microscopic shift vector $\mathbf{p}$ between the two sublattices (also known as *inner elasticity*). The physical moduli are those given above in equation (26a–26c).

S2 Detailed calculation of the pre-stress in the planar solution

We start by considering planar solutions, assuming that $w(R)$ is identically zero. The only unknown is the radial displacement $v(R)$. The Cauchy-Green tensor is given in the main text as

$$E_R = v'(R) + \frac{w'^2(R)}{2} \tag{28a}$$

$$E_\Theta = \frac{v(R)}{R}. \tag{28b}$$

The membrane stress tensor $\mathbf{S}$ has the same symmetry , and its eigenvalues S_R and S_Θ are given by the linear constitutive law associated with the quadratic stretching energy, $\mathbf{S} = \lambda\,\mathrm{tr}(\mathbf{E})\,\mathbf{I}_2 + 2\,\mu\,\mathbf{E}$:

$$\begin{pmatrix} S_R \\ S_\Theta \end{pmatrix} = \begin{pmatrix} 2\,\mu + \lambda & \lambda \\ \lambda & 2\,\mu + \lambda \end{pmatrix} \cdot \begin{pmatrix} E_R \\ E_\Theta \end{pmatrix}. \tag{29}$$

Combining the definition of the strain in equation (28b), the constitutive law (29) and the equation of equilibrium $\frac{1}{R}\frac{\mathrm{d}}{\mathrm{d}R}(R\,S_R) - \frac{S_\Theta}{R} = 0$, we find the equation $-\frac{v}{R} + v' + R\,v'' = 0$ whose solutions are linear combinations of the function R and $1/R$. Let us denote by $[\![f]\!]$ the jump $[\![f]\!] = f(R_1^+) - f(R_1^-)$ of a function f across the contractile circle at $R = R_1$. The solutions $v(R)$ of the differential equation which satisfy the condition at the center $v(0) = 0$, the clamping condition $v(R_2) = 0$ and the continuity at the contractile ring $[\![v]\!]_{R_1} = 0$ can be expressed in terms a single unknown amplitude $C = v(R_1)$ as

$$v(R) = \begin{cases} C\,\frac{R}{R_1} & \text{if } R < R_1 \\ \frac{C}{R_1\,(1-\alpha^2)}\,\left(R - \frac{R_2^2}{R}\right) & \text{if } R_1 < R < R_2, \end{cases} \tag{30}$$

where α denotes the radius of the domain relative to that of the contractile ring,

$$\alpha = \frac{R_2}{R_1}. \tag{31}$$

To find the parameter C, one can either minimize the total energy of the problem or use the balance of stress across the contractile ring (2D Young-Laplace equation):

$$[\![S_R]\!] - \frac{\Gamma}{R_1} = 0. \tag{32}$$

Both methods yield the same result, $C = -\frac{\alpha^2-1}{2\,\alpha^2}\,\frac{\Gamma}{\lambda+2\,\mu}$. In terms of Poisson's ratio $\nu = \frac{1}{1+\frac{2\,\mu}{\lambda}}$, this yields

$$C = -\frac{\alpha^2 - 1}{2\,\alpha^2}\,\frac{\nu\,\Gamma}{\lambda} \tag{33}$$

The corresponding stress can then be found from the constitutive law as

$$S_R = \begin{cases} -\frac{1+\nu}{2}\,S^* & \text{if } R < R_1 \\ \frac{S^*}{\alpha^2-1}\,\left(\frac{1+\nu}{2} + \frac{1-\nu}{2}\,\frac{\alpha^2}{(R/R_1)^2}\right) & \text{if } R_1 < R < R_2. \end{cases} \tag{34a}$$

$$S_\Theta = \begin{cases} -\frac{1+\nu}{2}\,S^* & \text{if } R < R_1 \\ \frac{S^*}{\alpha^2-1}\,\left(\frac{1+\nu}{2} - \frac{1-\nu}{2}\,\frac{\alpha^2}{(R/R_1)^2}\right) & \text{if } R_1 < R < R_2, \end{cases} \tag{34b}$$

where we have introduced the typical membrane stress S^*,

$$S^* = \frac{\alpha^2 - 1}{\alpha^2}\,\frac{\Gamma}{R_1}. \tag{35}$$

The stress in equation (34) is relevant to the planar (unbuckled) configuration. The planar configuration serves as the base solution of the forthcoming stability analysis, and in this context the stress will be referred to as *pre-stress*. The pre-stress is compressive in the interior region $R < R_1$, as $S_R = S_\Theta < 0$ there, and tensile in the outer region.

The pre-stress in equation (34) takes a particularly simple form in the limit $\nu = 1$ where the membrane preserves area (2D 'incompressibility', $\mu \ll \lambda$): then the stress is piecewise constant and isotropic,

$$S_R(R) = S_\Theta(R) = -S^*\, t(R) \tag{36}$$

where $t(R)$ is the piecewise function

$$t(R) = \begin{cases} 1 & \text{if } R < R_1 \\ -\frac{1}{\alpha^2-1} & \text{if } R_1 < R < R_2. \end{cases} \tag{37}$$

S3 Stability analysis of the axisymmetric plate

We solve the equations for the linear stability of a circular plate in axisymmetric geometry, driven by the contraction Γ of the embedded circle. The pre-stress is locally isotropic and piecewise constant, and writes $\mathbf{S} = -S^*\, t(R)\, \mathbf{I}_2$, where S^* is a typical stress defined in the main text. The classical equation for the linear stability of a circular plate [5, 7] has been recalled in the main text. In dimensionless form, it reads

$$-\frac{1}{\overline{R}}\,\frac{\mathrm{d}(\overline{R}\,q'(\overline{R}))}{\mathrm{d}\overline{R}} + \frac{q(\overline{R})}{\overline{R}^2} - \gamma\,\bar{t}(\overline{R})\,q(\overline{R}) = 0, \tag{38}$$

where $\overline{R} = R/R_1$ is the dimensionless radial coordinate which varies in the domain $0 < \overline{R} < \alpha$, the upper bound being the geometrical parameter $\alpha = \frac{R_2}{R_1}$, the quantity $q(\overline{R})$ is the radial slope, γ is the dimensionless buckling parameter defined in the main text as $\gamma = \frac{\Gamma R_1}{\beta}\,\frac{\alpha^2-1}{\alpha^2}$, and $\bar{t}(\overline{R})$ is the dimensionless form of the piecewise constant function entering in the distribution of pre-stress,

$$\bar{t}(\overline{R}) = \begin{cases} 1 & \text{if } 0 < \overline{R} < 1 \\ -\frac{1}{\alpha^2-1} & \text{if } 1 < \overline{R} < \alpha \end{cases}.$$

According to the method of linear stability analysis, the instability threshold $\gamma_\mathrm{c}(\alpha)$ is detected by the existence of a non-trivial solution $q(\overline{R})$ to equation (38) with the following boundary conditions: $q(0) = 0$ enforces the continuity of the slope at the center $\overline{R} = 0$, and $q(\alpha) = 0$ enforces the clamp condition on the outer boundary. This clamp condition assumes that the rotation is blocked along the outer boundary in the continuous model, and can be justified as follows. In the simulation of the vertex model, we use a *simple support* condition along the outer hexagonal boundary, *i.e.* we block the *position* of the outer set of vertices but let free the *rotation* of the adjacent edges. We observe that this *simple support* condition is equivalent to a *clamping* condition in the *axisymmetric* problem. Indeed, a finite slope $q(\alpha)$ on the circular edge of the perfectly axisymmetric plate implies a significant amount of stretching in the vertex model with hexagonal symmetry, especially near the corners of the hexagonal boundary. This stretching is zero when averaging over the azimuthal direction but is still associated with a high cost in elastic energy. For this reason, the rotation at the outer edge is effectively blocked. We have checked that the buckling modes of the vertex model indeed have a very small slope $q(\alpha)$ on the outer edge (after averaging in the azimuthal direction), as seen in the comparison of the mode shapes in figure 3C of the main text.

In both of the inner and outer regions $0 < \overline{R} < 1$ and $1 < \overline{R} < \alpha$, the dimensionless pre-stress $\gamma\,\bar{t}$ in equation (38) is constant and the generic solution q can be expressed as a combination of the Bessel function of the first kind J_1 and of the second kind, Y_1, as

$$\begin{aligned} q(\overline{R}) &= \mathcal{A}\, J_1\left(\sqrt{\gamma}\,\overline{R}\right) && \text{for } 0 < \overline{R} < 1 \\ q(\overline{R}) &= \mathcal{B}\, J_1\left(i\,\frac{\sqrt{\gamma}}{\sqrt{\alpha^2-1}}\,\overline{R}\right) + \mathcal{C}\, Y_1\left(i\,\frac{\sqrt{\gamma}}{\sqrt{\alpha^2-1}}\,\overline{R}\right) && \text{for } 1 < \overline{R} < \alpha. \end{aligned} \tag{39}$$

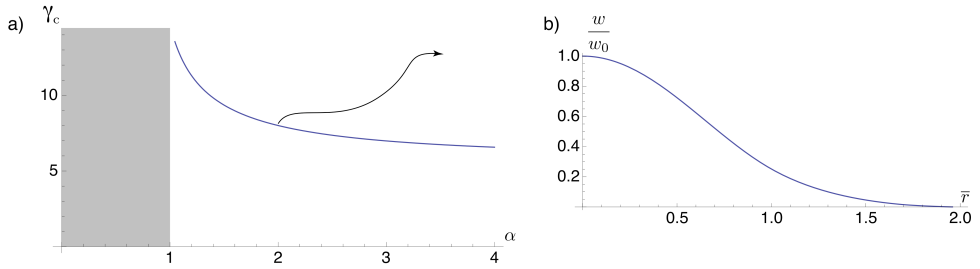

Figure S2: Linear stability analysis of an axisymmetric plate. (a) Dimensionless instability threshold γ_c as a function of the aspect-ratio α. (b) Normalized deflection of the buckling mode for $\alpha = 2$. The deflection w is reconstructed by integrating the slope q along the radial direction, $w(\overline{R}) \propto \int_0^{\overline{R}} q(\overline{R}')\,\mathrm{d}\overline{R}'$.

To avoid a singularity for $\overline{R} \to 0$, the coefficient of the function Y_1 that is divergent near zero has been set to zero in the inner region $0 < \overline{R} < 1$.

The constants $\mathcal{A}$, $\mathcal{B}$ and $\mathcal{C}$ are found from the conditions of continuity at $\overline{R} = 1$, and from the clamping condition $q(\alpha) = 0$,

$$q(1^-) = q(1^+) \tag{40a}$$
$$q'(1^-) = q'(1^+) \tag{40b}$$
$$q(\alpha) = 0 \tag{40c}$$

Here, equation (40a) warrants continuity of the radial slope $q \propto w'$ at the contractile circle and equation (40b) expresses the balance of moments across this contractile circle — note that the curvature q' in the radial direction is proportional to the internal moment. When above solutions for q are inserted, this yields a set of linear equations for the unknown coefficients

$$\mathbf{M}(\alpha, \gamma) \cdot \begin{pmatrix} \mathcal{A} \\ \mathcal{B} \\ \mathcal{C} \end{pmatrix} = \mathbf{0},$$

where the coefficients of the 3×3 matrix $\mathbf{M}(\alpha, \gamma)$ involve Bessel's functions and their derivatives. The buckling threshold is then given by the implicit equation

$$\det \mathbf{M}(\alpha, \gamma_c(\alpha)) = 0,$$

connecting α and γ. This equation is solved graphically in Fig. S2.

S4 Dependence of the buckling threshold on the bending modulus B

In figure S3, we show the dependence of the buckling threshold Γ_c on the bending modulus B for $(G, H) = (0.03514, 0)$, and for different geometries of the vertex model (symbols) having a constant ratio $P_2/P_1 = 2$, hence $\alpha \approx 2$. Datapoints nearly collapse onto the line plotted using Eq. [13] of the main text, featuring the typical values $\alpha = \frac{R_2}{R_1} = \frac{13.2}{6.9} = 1.91$ and $R_1 = 6.9$ from the vertex model. In the continuous model, we use linearized effective moduli since G is small and $H = 0$.

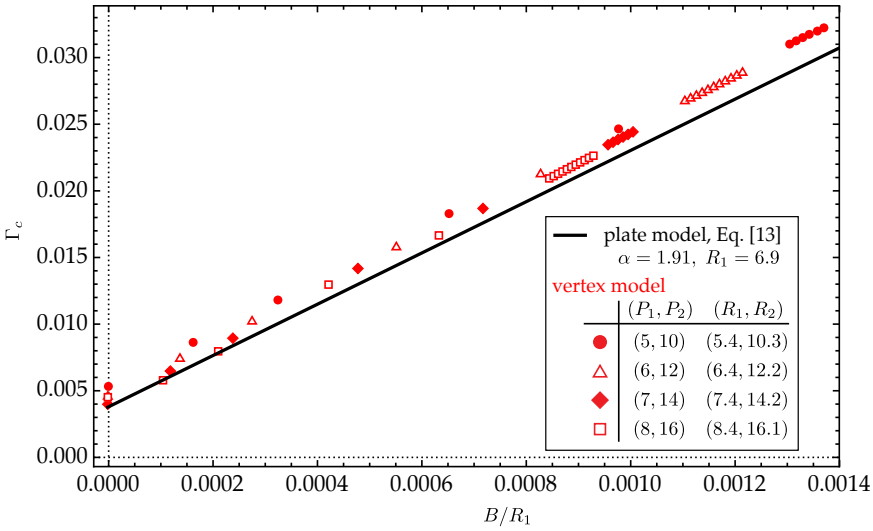

Figure S3: The buckling threshold Γ_c as a function of the bending modulus B, for $(G, H) = (0.03514, 0)$: comparison of the predictions of the vertex model for different geometries such that $P_2/P_1 = 2$, and of the continuous plate model. In the plate model, we use the linearized effective moduli $\beta_{\rm lin}$. The existence of a *residual* bending modulus is apparent from the fact that the threshold Γ_c is non-zero when $B = 0$. This residual bending modulus is accurately captured by the plate model, *i.e.* the black line does not pass through the origin.

S5 Comparison of the strain and stress maps: vertex model versus plate model

Here, we visualize the in-plane strain and stress corresponding to an equilibrium solution of the discrete vertex model, and compare them to the predictions of the continuous plate model.

To compute the strain $\mathbf{E}$ in a hexagonal mesh obtained from numerical simulations, we triangulate the mesh and calculate a constant strain on each triangle using the classical *constant strain element* (CST). Next, we evaluate its components $E_{RR} = \mathbf{e}_R \cdot \mathbf{E} \cdot \mathbf{e}_R$, $E_{\Theta\Theta} = \mathbf{e}_\Theta \cdot \mathbf{E} \cdot \mathbf{e}_\Theta$ and $E_{R\Theta} = \mathbf{e}_R \cdot \mathbf{E} \cdot \mathbf{e}_\Theta$ in the polar basis. In figure S4, the strain map is shown for $P_1 = 8$ internal layers (corresponding to $n_1 = 217$ cells inside the contractile hexagon), $P_2 = 16$ layers (corresponding to a total number of cells $n_2 = 817$), $G = 0.0351$, $H = 0$ (no perimeter term) and $\Gamma = 0.0217$. The discrete bending modulus B is set to $B = 0.00738$ such that this planar configuration is stable but very close to the buckling threshold.

The resulting strain is highly non-axisymmetric, as shown in Fig. S4. There is a large concentration of strain near the corners of the contractile hexagons – linear elasticity indeed predicts that the strain and stress diverge near these corners.

Averaging the strain and stress in the azimuthal direction Θ, one obtains much smoother profiles, see Fig. S5. As predicted by the smooth model, the averaged membrane stress is isotropic and homogeneous far from the contracting circle, both near the center and near the outer boundary. The values of this homogeneous and isotropic stress are well predicted by the smooth model (see figure).

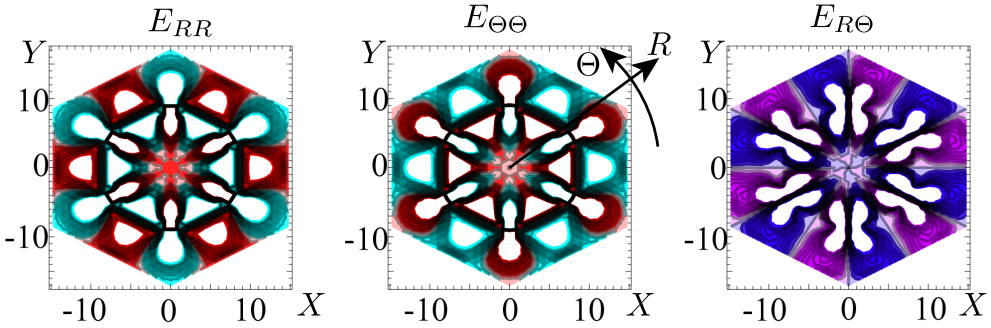

Figure S4: Map of the strain E_{RR}, $E_{\Theta\Theta}$, $E_{R\Theta}$ from the numerical simulation of the vertex model, pulled back in reference configuration (X, Y). Simulation parameters are listed in §S5. For E_{RR} and $E_{\Theta\Theta}$, the compressive stress is indicated in red, and tensile stress in blue. Out-of-range values are trimmed and shown in white. For $E_{R\Theta}$, our color code goes from blue to purple. Note that the strain is highly non-axisymmetric, with sharp singularities developing at the vertices of the hexagonal contour C. In spite of this, the analytical model based on an averaging in the Θ direction gives remarkably good results.

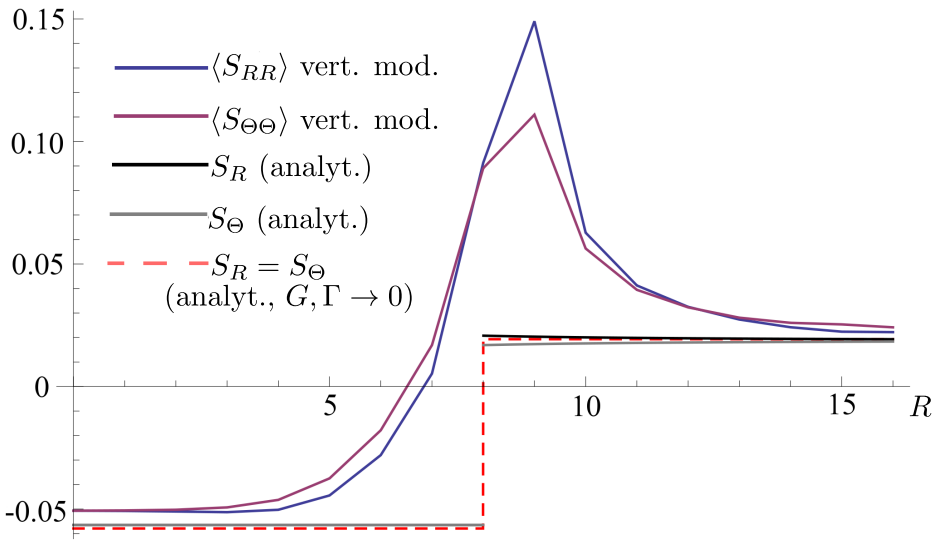

Figure S5: Comparison of the radial membrane stress $\langle S_{RR}\rangle$ and azimuthal membrane stress $\langle S_{\Theta\Theta}\rangle$ averaged over the azimuthal direction Θ from simulations of the vertex model simulation. The parameters are the same as in figure S4 and are listed in the text. This averaged stress is compared to the stress predicted by the axisymmetric plate model, both for finite G and Γ, see equation (34), and in the area-preserving limit $G, \Gamma \to 0$ in equation (36) (dashed piecewise constant curve).

S6 Mathematica code used for homogenization

Homogeneization of the vertex model for a hexagonal lattice by Fourier analysis

Basile Audoly
July 2014, last upated April 2015

Geometry and displacement

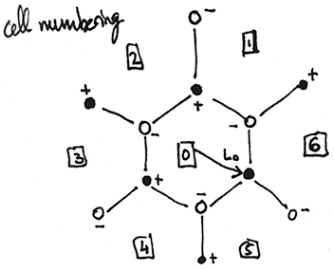

Centers of cells (central cell and adjacent ones) in reference configurations
Position of vertices in reference configuration: vertices are labelled by their relative position with respect to a cell (each vertex can be reached by the three adjacent cells)

```
cellRefCenter[cellIdx_] := Which[
    cellIdx === 0, {0, 0},
    cellIdx ≤ 6 && cellIdx > 0, (cellIdx * π/3 // {Cos[#], Sin[#]} &) L0 √3 ,
    True, Abort[]
  ];
vertexRefPos[cellIdx_, vertexIdx_] := If[
    vertexIdx > 0 && vertexIdx ≤ 6,
    L0 * (π/6 (2 vertexIdx - 1) // {Cos[#], Sin[#]} &) + cellRefCenter[cellIdx],
    Abort[]
  ];
```

```
(* check that vertex (0,1)=(5,3)=(6,5) *)
Map[Apply[vertexRefPos, #] &, {{0, 6}, {5, 2}, {6, 4}}] // Differences // Norm
```

```
0
```

```
(* graphic check *)
Graphics[Table[(Point[vertexRefPos[cellIdx, vertexIdx]] /. L0 → 1) //
    If[cellIdx == 0, {PointSize[.02], Gray, #}, {PointSize[.01], Orange, #}] &,
  {cellIdx, 0, 6}, {vertexIdx, 6}]]
```

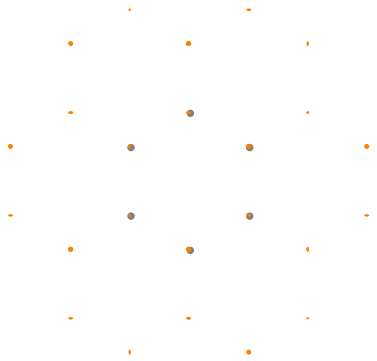

Real (r) and imaginary (i) parts of complex amplitudes for (u, v, w) (macrosopic displacement) and (p,q,s) (microscopic displacement

```
realAmplitudes = {ur, ui, vr, vi, pr, pi, qr, qi, wr, wi, sr, si}
```

```
{ur, ui, vr, vi, pr, pi, qr, qi, wr, wi, sr, si}
```

Deformed position given by x=a*X + Re((Umacro + Umicro) $e^{i\,\eta K.X}$), Umacro = $\begin{pmatrix} (u_r + i\,u_i)\,\eta \\ (v_r + i\,v_i)\,\eta \\ w_r + i\,w_i \end{pmatrix}$ and

Umicro = $\pm \frac{\eta^2}{2} \begin{pmatrix} p_r + i\,q_i \\ q_r + i\,q_i \\ s_r + i\,s_i \end{pmatrix}$

```
vertexDefPos[cellIdx_, vertexIdx_] := Module[{X, pm},
  X = vertexRefPos[cellIdx, vertexIdx];
  pm = (-1)^vertexIdx;
  (* alternating sign in microscopic displacement *)
  Append[a X, 0] + Re[{ (η (ur + i ui) + pm η^2 (pr + i pi)/2),
      (η (vr + i vi) + pm η^2 (qr + i qi)/2), ((wr + i wi) + pm η^2 (sr + i si)/2)} * e^(i η {kx,ky}.X)] //
   Simplify[FunctionExpand[# /. Re[a_ b_] :> Re[Expand[a b]]] // ExpToTrig,
     η ∈ Reals && kx ∈ Reals && ky ∈ Reals && L0 ∈ Reals &&
      (And @@ Map[# ∈ Reals &, realAmplitudes])] &
 ]
```

```
(* example *)
vertexDefPos[0, 6]
```

$$\left\{\frac{1}{2}\left(\sqrt{3}\ \mathtt{a}\ \mathtt{L0}+\eta\ (2\ \mathtt{ur}+\mathtt{pr}\ \eta)\ \mathtt{Cos}\left[\frac{1}{2}\left(\sqrt{3}\ \mathtt{kx}-\mathtt{ky}\right)\ \mathtt{L0}\ \eta\right]-\right.\right.$$
$$\left.\eta\ (2\ \mathtt{ui}+\mathtt{pi}\ \eta)\ \mathtt{Sin}\left[\frac{1}{2}\left(\sqrt{3}\ \mathtt{kx}-\mathtt{ky}\right)\ \mathtt{L0}\ \eta\right]\right),$$
$$\frac{1}{2}\left(-\mathtt{a}\ \mathtt{L0}+\eta\ (2\ \mathtt{vr}+\mathtt{qr}\ \eta)\ \mathtt{Cos}\left[\frac{1}{2}\left(\sqrt{3}\ \mathtt{kx}-\mathtt{ky}\right)\ \mathtt{L0}\ \eta\right]-\right.$$
$$\left.\eta\ (2\ \mathtt{vi}+\mathtt{qi}\ \eta)\ \mathtt{Sin}\left[\frac{1}{2}\left(\sqrt{3}\ \mathtt{kx}-\mathtt{ky}\right)\ \mathtt{L0}\ \eta\right]\right),$$
$$\left.\frac{1}{2}\left((2\ \mathtt{wr}+\mathtt{sr}\ \eta^2)\ \mathtt{Cos}\left[\frac{1}{2}\left(\sqrt{3}\ \mathtt{kx}-\mathtt{ky}\right)\ \mathtt{L0}\ \eta\right]-(2\ \mathtt{wi}+\mathtt{si}\ \eta^2)\ \mathtt{Sin}\left[\frac{1}{2}\left(\sqrt{3}\ \mathtt{kx}-\mathtt{ky}\right)\ \mathtt{L0}\ \eta\right]\right)\right\}$$

```
(* check that vertex (0,1)=(5,3)=(6,5) match in deformed configuration *)
Map[Apply[vertexDefPos, #] &, {{0, 6}, {5, 2}, {6, 4}}] // Differences // Norm
```

```
0
```

Definition of area vector A_k

```
AkVector[cellIdx_] :=
 Table[vertexDefPos[cellIdx, vertexIdx], {vertexIdx, 6}] // Append[
          #, First[#]] & // {Most[#], Rest[#]} & // Transpose //
     Map[1/2 #[[1]] × #[[2]] &, #] & // Total // Series[#, {η, 0, 4}] & // Simplify
```

L0 such that reference area is A0=1, based on the formula for the area of an hexagon

```
L0Rule = {L0 → Sqrt[2/(3 Sqrt[3])]};
```

Compute area vector, scalar area and unit normal for the central and 6 peripheral cells

```
ProcessSevenCells = Table[
   Module[{akv, aks, nk},
    Print["Processing cell #", cellIdx, "..."];
    akv = AkVector[cellIdx];
    aks = akv // Norm // # /. Abs[u_]^2 :> u^2 & // Simplify[#, a > 0 && L0 > 0] &;
    nk = akv/aks // Simplify[# /. L0Rule] &;
    <|"vector" → akv, "scalar" → aks, "normal" → nk|>
   ],
   {cellIdx, 0, 6}];
processedCentralCell = ProcessSevenCells[[1]];
processedPeriphCells = ProcessSevenCells[[2 ;; -1]];
```

```
Processing cell #0...
Processing cell #1...
Processing cell #2...
Processing cell #3...
Processing cell #4...
Processing cell #5...
Processing cell #6...
```

Energy terms

Terms involving area

```
areaTerm =
 processedCentralCell // 1/2 (#[["scalar"]] - 1)^2 & // Simplify[# /. L0Rule, a > 0] &
```

$$\frac{1}{2}\left(-1+a^2\right)^2-\frac{1}{2}\left(\left(-1+a^2\right)\left(2\,a\left(kx\,ui+ky\,vi\right)-\left(kx^2+ky^2\right)wi^2\right)\right)\eta^2+$$
$$\frac{1}{8}\left(\left(-2\,a\left(kx\,ui+ky\,vi\right)+\left(kx^2+ky^2\right)wi^2\right)^2+\right.$$
$$\frac{1}{9\,a^2}\left(-1+a^2\right)\left(3^{1/4}\,a^3\left(2\times 3^{1/4}\,kx^3\,ui+2\,kx\,ky\left(3\sqrt{2}\,pr+3^{1/4}\,ky\,ui\right)+ky^2\left(-3\sqrt{2}\,qr+\right.\right.\right.$$
$$\left.\left.\left.2\times 3^{1/4}\,ky\,vi\right)+kx^2\left(3\sqrt{2}\,qr+2\times 3^{1/4}\,ky\,vi\right)\right)-2\sqrt{3}\,a^2\left(kx^2+ky^2\right)^2wi^2+\right.$$
$$\left.36\,a\left(kx^2+ky^2\right)\left(kx\,ui+ky\,vi\right)wi^2-9\left(kx^2+ky^2\right)^2wi^4\right)\Bigg)\eta^4+O[\eta]^5$$

```
normalsDotTerm = Map[1 - (processedCentralCell[["normal"]]).(#[["normal"]]) &,
    processedPeriphCells] // Simplify //
  (*the coefficient 2 is because each edge is counted twice
   (one for each adjacent face) *) B/2 * Total[#] & // Simplify[# /. L0Rule] &
```

$$\frac{\sqrt{3}\,B\left(kx^2+ky^2\right)^2wr^2\,\eta^4}{2\,a^2}+O[\eta]^5$$

Terms involving segment lengths

```
meanEdgeLength =
 Map[Norm, Table[vertexDefPos[0, vertexIdx], {vertexIdx, 6}] // Append[
     #, First[#]] & // Differences] // # /. Abs → Identity & //
   Series[#, {η, 0, 4}] & // Mean // Simplify[# /. L0Rule, a > 0] &
```

$$\frac{\sqrt{2}\,a}{3^{3/4}}+\frac{\left(-2\,a\left(kx\,ui+ky\,vi\right)+\left(kx^2+ky^2\right)wi^2\right)\eta^2}{2\sqrt{2}\,3^{3/4}\,a}+$$
$$\frac{1}{288\sqrt{2}\,3^{1/4}\,a^3}\left(4\,a^3\left(2\,kx^3\,ui+2\,kx\,ky\left(\sqrt{2}\,3^{3/4}\,pr+ky\,ui\right)+\right.\right.$$
$$ky^2\left(-\sqrt{2}\,3^{3/4}\,qr+2\,ky\,vi\right)+kx^2\left(\sqrt{2}\,3^{3/4}\,qr+2\,ky\,vi\right)\Big)+$$
$$36\times 3^{1/4}\,a\left(3^{1/4}\,kx^3\,ui+kx\,ky\left(-2\sqrt{2}\,pr+3^{1/4}\,ky\,ui\right)+kx^2\left(-\sqrt{2}\,qr+3^{1/4}\,ky\,vi\right)+\right.$$
$$\left.ky^2\left(\sqrt{2}\,qr+3^{1/4}\,ky\,vi\right)\right)wi^2-9\sqrt{3}\left(kx^2+ky^2\right)^2wi^4+$$
$$2\,a^2\left(108\,pr^2+108\,qr^2+216\,sr^2+6\sqrt{3}\,kx^2\,ui^2+18\sqrt{3}\,ky^2\,ui^2-\right.$$
$$24\sqrt{3}\,kx\,ky\,ui\,vi+18\sqrt{3}\,kx^2\,vi^2+6\sqrt{3}\,ky^2\,vi^2+$$
$$36\sqrt{2}\,3^{1/4}\,pr\left(ky\,ui+kx\,vi\right)+36\sqrt{2}\,3^{1/4}\,qr\left(kx\,ui-ky\,vi\right)-4\,kx^4\,wi^2-$$
$$\left.\left.8\,kx^2\,ky^2\,wi^2-4\,ky^4\,wi^2+3\,kx^4\,wr^2+6\,kx^2\,ky^2\,wr^2+3\,ky^4\,wr^2\right)\right)\eta^4+O[\eta]^5$$

```
{lineTensionTerm, perimeterTerm} =
  {G * 6/2 * meanEdgeLength, H/2 * (6 meanEdgeLength)^2} // Simplify;
```

Assembling

```
allTerms = areaTerm + lineTensionTerm + perimeterTerm + normalsDotTerm // Simplify
```

$$\left(\frac{1}{2}\left(-1+a^2\right)^2+\sqrt{2}\ 3^{1/4}\ a\ G+4\ \sqrt{3}\ a^2\ H\right)-\frac{\left(\left(2\ a^3+\sqrt{2}\ 3^{1/4}\ G+a\left(-2+8\ \sqrt{3}\ H\right)\right)\ \left(2\ a\ \left(kx\ ui+ky\ vi\right)-\left(kx^2+ky^2\right)\ wi^2\right)\right)\ \eta^2}{4\ a}+$$

$$\frac{1}{576}\left(72\ \left(\left(-2\ a\ \left(kx\ ui+ky\ vi\right)+\left(kx^2+ky^2\right)\ wi^2\right)^2+\frac{1}{9\ a^2}\left(-1+a^2\right)\ \left(3^{1/4}\ a^3\ \left(2\times 3^{1/4}\ kx^3\ ui+2\ kx\ ky\ \left(3\ \sqrt{2}\ pr+3^{1/4}\ ky\ ui\right)+ky^2\ \left(-3\ \sqrt{2}\ qr+2\times 3^{1/4}\ ky\ vi\right)+kx^2\ \left(3\ \sqrt{2}\ qr+2\times 3^{1/4}\ ky\ vi\right)\right)-2\ \sqrt{3}\ a^2\ \left(kx^2+ky^2\right)^2\ wi^2+36\ a\ \left(kx^2+ky^2\right)\ \left(kx\ ui+ky\ vi\right)\ wi^2-9\ \left(kx^2+ky^2\right)^2\ wi^4\right)\right)+\frac{288\ \sqrt{3}\ B\ \left(kx^2+ky^2\right)^2\ wr^2}{a^2}+\frac{1}{a^3}\sqrt{2}\ 3^{3/4}\ G\ \left(4\ a^3\ \left(2\ kx^3\ ui+2\ kx\ ky\ \left(\sqrt{2}\ 3^{3/4}\ pr+ky\ ui\right)+ky^2\ \left(-\sqrt{2}\ 3^{3/4}\ qr+2\ ky\ vi\right)+kx^2\ \left(\sqrt{2}\ 3^{3/4}\ qr+2\ ky\ vi\right)\right)+36\times 3^{1/4}\ a\ \left(3^{1/4}\ kx^3\ ui+kx\ ky\ \left(-2\ \sqrt{2}\ pr+3^{1/4}\ ky\ ui\right)+kx^2\ \left(-\sqrt{2}\ qr+3^{1/4}\ ky\ vi\right)+ky^2\ \left(\sqrt{2}\ qr+3^{1/4}\ ky\ vi\right)\right)\ wi^2-9\ \sqrt{3}\ \left(kx^2+ky^2\right)^2\ wi^4+2\ a^2\ \left(108\ pr^2+108\ qr^2+216\ sr^2+6\ \sqrt{3}\ kx^2\ ui^2+18\ \sqrt{3}\ ky^2\ ui^2-24\ \sqrt{3}\ kx\ ky\ ui\ vi+18\ \sqrt{3}\ kx^2\ vi^2+6\ \sqrt{3}\ ky^2\ vi^2+36\ \sqrt{2}\ 3^{1/4}\ pr\ \left(ky\ ui+kx\ vi\right)+36\ \sqrt{2}\ 3^{1/4}\ qr\ \left(kx\ ui-ky\ vi\right)-4\ kx^4\ wi^2-8\ kx^2\ ky^2\ wi^2-4\ ky^4\ wi^2+3\ kx^4\ wr^2+6\ kx^2\ ky^2\ wr^2+3\ ky^4\ wr^2\right)\right)+\frac{1}{a^2}24\ H\ \left(4\ a^3\ \left(2\ kx^3\ ui+2\ kx\ ky\ \left(\sqrt{2}\ 3^{3/4}\ pr+ky\ ui\right)+ky^2\ \left(-\sqrt{2}\ 3^{3/4}\ qr+2\ ky\ vi\right)+kx^2\ \left(\sqrt{2}\ 3^{3/4}\ qr+2\ ky\ vi\right)\right)+12\times 3^{1/4}\ a\ \left(3^{1/4}\ kx^3\ ui+kx\ ky\ \left(-6\ \sqrt{2}\ pr+3^{1/4}\ ky\ ui\right)+kx^2\ \left(-3\ \sqrt{2}\ qr+3^{1/4}\ ky\ vi\right)+ky^2\ \left(3\ \sqrt{2}\ qr+3^{1/4}\ ky\ vi\right)\right)\ wi^2-3\ \sqrt{3}\ \left(kx^2+ky^2\right)^2\ wi^4+2\ a^2\ \left(108\ pr^2+108\ qr^2+216\ sr^2+18\ \sqrt{3}\ kx^2\ ui^2+18\ \sqrt{3}\ ky^2\ ui^2+18\ \sqrt{3}\ kx^2\ vi^2+18\ \sqrt{3}\ ky^2\ vi^2+36\ \sqrt{2}\ 3^{1/4}\ pr\ \left(ky\ ui+kx\ vi\right)+36\ \sqrt{2}\ 3^{1/4}\ qr\ \left(kx\ ui-ky\ vi\right)-4\ kx^4\ wi^2-8\ kx^2\ ky^2\ wi^2-4\ ky^4\ wi^2+3\ kx^4\ wr^2+6\ kx^2\ ky^2\ wr^2+3\ ky^4\ wr^2\right)\right)\right)\eta^4+O[\eta]^5$$

Define energy for homogeneous transformations

```
w = allTerms // Normal // # /. η → 0 & // Function @@ {a, #} &
```

$$\text{Function}\left[a,\ \frac{1}{2}\left(-1+a^2\right)^2+\sqrt{2}\ 3^{1/4}\ a\ G+4\ \sqrt{3}\ a^2\ H\right]$$

Equation for a definition confirguration PE (planar equilibrium)

```
-w'[a]/(2 a) // Simplify
```

$$1 - a^2 - \frac{3^{1/4}\, G}{\sqrt{2}\, a} - 4\sqrt{3}\, H$$

Let us define $\tilde{G}$ which incoporates some numerical factors into G for convenience

```
Needs["Notation`"];
Symbolize[ G̃ ];
toGt = {G → a √2 G̃ / 3^(1/4)};
-w'[a]/(2 a) /. toGt // Simplify
```

$$1 - a^2 - \tilde{G} - 4\sqrt{3}\, H$$

```
(* spin-like matrices *)
Sx = {{0, 1}, {1, 0}};
Sy = {{1, 0}, {0, -1}};
S = {Sx, Sy};
SDoubleContract[t_] := TensorContract[S⊗t, {{2, 4}, {3, 5}}];
```

We simplified the total energy manually and came up with the expression below, which we check for correctness (notice that result is zero)

```
KdotVim = kx ui + ky vi;
KSq = kx^2 + ky^2;
KVec = {kx, ky};
QreVec = {pr, qr};
VimVec = {ui, vi};
allTerms - (
    w[a] + w'[a]/(2 a) (- a KdotVim + 1/2 KSq wi^2) η^2 +
     + (w'[a]/(24 Sqrt[3]) (KSq KdotVim - KSq^2/a wi^2 + 3^(3/4)/Sqrt[2] QreVec.SDoubleContract[KVec⊗KVec]) +
          (2 a^2 - G̃)/4 KdotVim^2
          + (1/4 G̃ + Sqrt[3] H) (3/2 KSq VimVec.VimVec + 3 Sqrt[3] (QreVec.QreVec + 2 sr^2) +
               Sqrt[2] 3^(3/4) QreVec.SDoubleContract[KVec⊗ (VimVec - 1/(2 a) wi^2 KVec)]) +
          1/(8 a^2) (1 - 3/4 G̃ - Sqrt[3] H) (-4 a KSq KdotVim wi^2 + KSq^2 wi^4) +
          1/(4 Sqrt[3]) (G̃/4 + Sqrt[3] H + 6 B/a^2) KSq^2 wr^2
        ) η^4
    ) // Simplify[# /. toGt] &
O[η]^5
```

Cauchy-Green strain

Deformation gradient

```
Fsmooth = a {X, Y, 0} + Re[{η (ur + i ui), η (vr + i vi), (wr + i wi)} * e^(i η {kx,ky}.{X,Y})] //
        ExpToTrig // # /. Re[a_ b_] :> Re[Expand[a b]] & //
      Simplify[#, kx ∈ Reals && ky ∈ Reals && η ∈ Reals && X ∈ Reals &&
          Y ∈ Reals && (And @@ Map[# ∈ Reals &, realAmplitudes])] & //
     {D[#, X], D[#, Y]} & // Transpose;
Fsmooth // MatrixForm
```

$$\begin{pmatrix} a - kx\,ui\,\eta^2 \cos[kx\,X\,\eta + ky\,Y\,\eta] - kx\,ur\,\eta^2 \sin[kx\,X\,\eta + ky\,Y\,\eta] & -ky\,ui\,\eta^2 \cos[kx\,X\,\eta + ky\,Y\,\eta] \\ -kx\,vi\,\eta^2 \cos[kx\,X\,\eta + ky\,Y\,\eta] - kx\,vr\,\eta^2 \sin[kx\,X\,\eta + ky\,Y\,\eta] & a - ky\,vi\,\eta^2 \cos[kx\,X\,\eta + ky\,Y\,\eta] \\ -kx\,wi\,\eta \cos[kx\,X\,\eta + ky\,Y\,\eta] - kx\,wr\,\eta \sin[kx\,X\,\eta + ky\,Y\,\eta] & -ky\,wi\,\eta \cos[kx\,X\,\eta + ky\,Y\,\eta] \end{pmatrix}$$

Cauchy - Green strain at origin

```
Eo = Transpose[Fsmooth].Fsmooth //
   Simplify[(# - a^2 IdentityMatrix[2])/(2 a) /. {X → 0, Y → 0}] &
```

$$\left\{\left\{\frac{kx\,\eta^2\left(-2\,a\,ui+kx\left(wi^2+\left(ui^2+vi^2\right)\eta^2\right)\right)}{2\,a},\ \frac{\eta^2\left(-a\left(ky\,ui+kx\,vi\right)+kx\,ky\left(wi^2+\left(ui^2+vi^2\right)\eta^2\right)\right)}{2\,a}\right\},\ \left\{\frac{\eta^2\left(-a\left(ky\,ui+kx\,vi\right)+kx\,ky\left(wi^2+\left(ui^2+vi^2\right)\eta^2\right)\right)}{2\,a},\ \frac{ky\,\eta^2\left(-2\,a\,vi+ky\left(wi^2+\left(ui^2+vi^2\right)\eta^2\right)\right)}{2\,a}\right\}\right\}$$

Check of formula for E(0, 0) proposed in SI

```
-η^2 {ui, vi}⊗{kx, ky} + η^2/(2 a) {kx, ky}⊗{kx, ky} (η^2 (ui^2 + vi^2) + wi^2) //
   (# + Transpose[#])/2 & // Simplify[Eo - #] &
```

$$\{\{0, 0\}, \{0, 0\}\}$$

Identification of expansion at order 2

Cancellation of the η^2 term in the energy follows from the condition w'(a)=0 used earlier

```
allTerms - (w'[a]/2 Tr[Eo]) // Normal // CoefficientList[#, η] & // #[[3]] & //
   # /. toGt & // Simplify
```

$$0$$

Identification of expansion at order 4

```
elimG = Solve[w'[a] == 0, G] // First
```

$$\left\{G \to -\frac{\sqrt{2}\left(-a+a^3+4\sqrt{3}\,a\,H\right)}{3^{1/4}}\right\}$$

```
(* now  G̃ as a function of a *)
Solve[(G /. elimG) == (G /. toGt), G̃]
```

$$\left\{\left\{\tilde{G} \to 1-a^2-4\sqrt{3}\,H\right\}\right\}$$

```
coefsDirectMethod =
  allTerms - (w[a] + 1/2 λStar Tr[Eo]^2 + μStar Tr[Eo.Eo] + β/2 η^4 (kx^2 + ky^2)^2 wr^2 +
                τ/2 η^4 (pr^2 + qr^2 + 2 sr^2) - γ η^2 {pr, qr}.SDoubleContract[Eo]) //
           Expand[# /. elimG] & // CoefficientList[#, {kx, ky, ui, vi, wi,
             wr, pr, qr, sr}] & // Flatten // Union // Map[# == 0 &, #] & //
     Simplify // Solve[#, {λStar, μStar, β, τ, γ}] & // Simplify
```

$$\left\{\left\{\lambda\text{Star} \to \frac{1}{4}\left(-5+9\,a^2+8\sqrt{3}\,H\right),\ \mu\text{Star} \to -\frac{3}{4}\left(-1+a^2\right),\right.\right.$$
$$\left.\left.\beta \to \frac{a^2-a^4+24\,B}{8\sqrt{3}\,a^2},\ \tau \to -\frac{3}{2}\sqrt{3}\left(-1+a^2\right),\ \gamma \to -\frac{3^{3/4}\left(-1+a^2\right)}{2\sqrt{2}}\right\}\right\}$$

Relaxing the microscopic displacement δ

Check formulas calculated by hand for optimum of energy with respect to {δxr, δyr}

```
CauchyGreenFormal = Array[CGf, {2, 2}] /. CGf[1, 2] → CGf[2, 1]
 (* a symmetric matrix *);
```

A useful identity

```
(SDoubleContract[CauchyGreenFormal] // #.# &) -
   (- Tr[CauchyGreenFormal]^2 + 2 Tr[CauchyGreenFormal.CauchyGreenFormal]) //
 (*Solve[#==0,{α,β}]&//*)Simplify
```

0

```
microEnergy = τ/2 (pr^2 + qr^2) - γ Tr[CauchyGreenFormal.S.{pr, qr}];
(* as found above by identification *)
microOptimum = {{pr, qr}, γ/τ SDoubleContract[CauchyGreenFormal]} // Transpose //
   Map[Rule @@ # &, #] &;
(* check that this value of δ is the optimum *)
Table[D[microEnergy, δ], {δ, {pr, qr}}] /. microOptimum // Simplify
```

{0, 0}

Optimum value of the energy

```
(microEnergy /. microOptimum) -
   (-γ^2/(2 τ) (SDoubleContract[CauchyGreenFormal] // #.# &)) // Simplify
```

0

Same quantity, rewritten in terms of invariants

```
(microEnergy /. microOptimum) -
   (-γ^2/(2 τ) (-Tr[CauchyGreenFormal]^2 + 2 Tr[CauchyGreenFormal.CauchyGreenFormal])) //
 Simplify
```

0

```
γ^2/τ /. coefsDirectMethod(* numerical value of the coefficient —
  mind the factor 1/2, which has been left out *)
```

$\left\{\frac{1}{4}\left(1 - a^2\right)\right\}$

```
renormalizedCoefs =
 1/2 λ Tr[CauchyGreenFormal]^2 + μ Tr[CauchyGreenFormal.CauchyGreenFormal] - γ^2/(2 τ)
      (-Tr[CauchyGreenFormal]^2 + 2 Tr[CauchyGreenFormal.CauchyGreenFormal]) // <|
     λrenorm → 2 * Coefficient[#, Tr[CauchyGreenFormal]^2], μrenorm →
      Coefficient[#, Tr[CauchyGreenFormal.CauchyGreenFormal]]|> & // Expand
```

$\left\langle\left|\lambda\text{renorm} \to 2\left(\frac{\lambda}{2} + \frac{\gamma^2}{2\,\tau}\right), \mu\text{renorm} \to \mu - \frac{\gamma^2}{\tau}\right|\right\rangle$

```
renormalizedCoefsFinal = renormalizedCoefs /. coefsDirectMethod // Simplify
```

$$\left\{\left\langle\left|\lambda\text{renorm}\to 2\left(\frac{1}{8}\left(1-\text{a}^2\right)+\frac{1}{8}\left(-5+9\,\text{a}^2+8\sqrt{3}\,\text{H}\right)\right),\ \mu\text{renorm}\to\frac{1}{2}\left(1-\text{a}^2\right)\right|\right\rangle\right\}$$

Linearized moduli (a is close to 1, and H and B are small)

Listed in main text, equation 9

```
{G /. elimG,
      λrenorm /. renormalizedCoefsFinal,
      μrenorm /. renormalizedCoefsFinal,
      β /. coefsDirectMethod,
      λrenorm / (2 μrenorm + λrenorm) (* Poisson's coef *) /. renormalizedCoefsFinal} /.
    {a → 1 - η OneMinusA, H → η HH, B → η BB} //
   Flatten // Series[#, {η, 0, 1}] & // Normal
```

$$\left\{\left(-4\sqrt{2}\,3^{1/4}\,\text{HH}+\frac{2\sqrt{2}\,\text{OneMinusA}}{3^{1/4}}\right)\eta,\ 1+\left(2\sqrt{3}\,\text{HH}-4\,\text{OneMinusA}\right)\eta,\right.$$
$$\left.\text{OneMinusA}\,\eta,\ \left(\sqrt{3}\,\text{BB}+\frac{\text{OneMinusA}}{4\sqrt{3}}\right)\eta,\ 1-2\,\text{OneMinusA}\,\eta\right\}$$

References

[1] M. Arroyo and T. Belytschko. An atomistic-based finite deformation membrane for single-layer crystalline films. *Journal of the Mechanics and Physics of Solids*, 50:1941—1977, 2002.

[2] M. Arroyo and T. Belytschko. Finite crystal elasticity of carbon nanotubes based on the exponential cauchy-born rule. *Physical Review B (Condensed Matter and Materials Physics)*, 69:115415, 2004.

[3] B. Audoly and Y. Pomeau. Elasticity and geometry. In R. Kaiser and J. Montaldi, editors, *Peyresq Lecture Notes on Nonlinear Phenomena*, chapter 1, pages 1–35. World Scientific, 2000.

[4] C. S. G. Cousins. Inner elasticity. *Journal of Physics C: Solid State Physics*, 11:4867–4879, 1978.

[5] J. W. Hutchinson and Z. Suo. Mixed mode cracking in layered materials. *Advances in Applied Mechanics*, 29:63–191, 1992.

[6] D.B. Staple, R. Farhadifar, J.-C. Röper, B. Aigouy, S. Eaton, and F. Jülicher. Mechanics and remodelling of cell packings in epithelia. *The European Physical Journal E*, 33(2):117–127, 2010.

[7] S. Timoshenko and J. M. Gere. *Theory of elastic stability*. MacGraw Hill, New York, 2$^{\text{nd}}$ edition, 1961.

[8] Wolfram Research, Inc. Mathematica edition: Version 10.0. Champaign, IL (USA), 2014.

[9] J. Wu, K. C. Hwang, and Y. Huang. An atomistic-based finite-deformation shell theory for single-wall carbon nanotubes. *Journal of the Mechanics and Physics of Solids*, 56(1):279–292, 2008.